frontiers | Frontiers in Earth Science

TYPE Original Research
PUBLISHED 28 March 2025
DOI 10.3389/feart.2025.1497600

OPEN ACCESS

EDITED BY
George Kontakiotis,
National and Kapodistrian University of Athens, Greece

REVIEWED BY
Hamad Ur Rahim,
Pakistan Museum of Natural History, Pakistan
Merve Ozyurt,
Karadeniz Technical University, Türkiye

*CORRESPONDENCE
Kun Tian,
973353569@qq.com

RECEIVED 17 September 2024
ACCEPTED 25 February 2025
PUBLISHED 28 March 2025

CITATION
Tian K, Zhou J, Yin X, Xue C, Cao J, Ma L and Zhao W (2025) Characteristics and the formation mechanism of the dolomite reservoirs for Lower Ordovician Majiagou Formation, central Ordos Basin, China. *Front. Earth Sci.* 13:1497600. doi: 10.3389/feart.2025.1497600

Characteristics and the formation mechanism of the dolomite reservoirs for Lower Ordovician Majiagou Formation, central Ordos Basin, China

Kun Tian[1]*, Jinsong Zhou[1], Xiao Yin[1], Chunqi Xue[2], Jun Cao[1], Ling Ma[1] and Weibo Zhao[1]

[1]Natural Gas Research Institute of Shaanxi Yanchang Petroleum Group Co., Ltd., Xi'an, China, [2]PetroChina Changqing Oilfield Company, Xi'an, China

The distribution of anhydrite contributes to the formation of high-quality dolomite reservoirs. However, the lower part of the Lower Ordovician Majiagou Formation in the central Ordos Basin shows significant natural gas potential despite in anhydrite-depleted settings. Therefore, its formation mechanism is crucial for carbonate hydrocarbon exploration in evaporite-depleted regions globally. Through integrated multidisciplinary analysis (petrography, cathodoluminescence (CL), X-ray diffraction (XRD) and carbon (C)-oxygen (O)-strontium (Sr) isotopes), the sedimentary-diagenetic differentiation mechanism of dolomite reservoirs in the study area was revealed. Two types of dolomite mainly develop in the study area. (Very) finely dolomite (Md1) is composed by micritic or microcrystalline (<20 μm), euhedral to subhedral dolomite crystals with laminated structure observed, the CL shows a very dull or dark red in color, low order degree (0.65 on average), a positive $\delta^{13}C$ shift (+0.83‰ on average), high Sr isotope ratio ($^{87}Sr/^{86}Sr$ = 0.70967 on average) and paleosalinity Z value (125.9747 on average). Fine-medium crystalline dolomite (Md2) is composed by finely or medium crystalline (20-60 μm), euhedral to subhedral dolomite crystals, the dark red or orange in color by CL analysis, high order degree (0.85 on average), a negative $\delta^{18}O$ shift (–7.12‰ on average), low Sr isotope ratio ($^{87}Sr/^{86}Sr$ = 0.70946 on average) and paleosalinity Z value (122.8781 on average). It is indicated that Md1 formed in a restricted platform tidal flat environment with weak hydrodynamic conditions, during the syngenetic-quasi syngenetic stages through the seepage reflux of high-salinity seawater in an open, low-oxidation, low-temperature environment. Md2 formed through the superimposed transformation of the original tidal flat shoal during the shallow burial stage, driven by the reflux of reducing seawater in a closed, low-reduction, higher-temperature environment. In addition, the atmospheric freshwater dissolution and the enhanced euhedral growth of dolomite crystals during the burial stage promote the development of high-quality reservoirs. This study provides novel geochemical and sedimentary insights for predicting

dolomite reservoirs in anhydrite-depleted settings, aiding global hydrocarbon exploration in similar basins.

KEYWORDS

dolomitization, diagenesis of dolomite reservoir, majiagou formation, wuqi area, ordos basin

1 Introduction

The genesis of dolomite reservoirs has consistently been a topical issue. The formation of large-scale dolomite reservoirs is controlled by dolomitization models, which is closely related to sedimentary environment, the origin of Mg^{2+}, hydrodynamic mechanism, etc (Jones and Xiao, 2005; Warren, 2000). In recent years, various models for dolomitization have been proposed to account for the ubiquitous occurrences of dolomite, such as evaporative, seepage–reflux, mixing zone, burial, hydrothermal, and microbial mechanisms (Hsü and Schneider, 1973; Garven et al., 1999; Davies and Smith, 2006; Bontognali et al., 2012; Özyurt et al., 2023; Özyurt and Kırmacı, 2024; Rahim et al., 2022; Kırmacı et al., 2018), making the development of new basis for the prediction of effective reservoir distribution.

Ordos Basin is the second largest gas producing basin in China, and the middle part of the basin develops the carbonate gas reservoir of the Middle Ordovician Majiagou Formation, covering an area of about $4.8 \times 10^4 km^2$ (Shi et al., 2009). Majiagou Formation is a set of carbonate-dominated strata containing evaporite, which can be divided into six sections from bottom to top. Among them, the fifth member of Majiagou Formation can be divided into 10 sub-members from top to bottom (Yu et al., 2012; Zhu et al., 2014). Since the end of the 20th century, the Jingbian gas field with high production has been discovered in sub-member $M5^1$ to $M5^4$ of Majiagou Formation. Recently, more than one million cubic meters of gas production per day are discovered in the $M5^5$ to $M5^{10}$ sub-members of Majiagou Formation, which proves the high gas production capacity of this formation (Shi et al., 2013; Wu et al., 2014; Huang et al., 2011; Yang et al., 2014; Huang and Bao, 2012).

Due to the high gas production in the Majiagou Formation of Ordos Basin, numerous models for dolomitization has been proposed including mixed-water dolomitization (Zhao et al., 2005), quasi syngenetic dolomitization (Han and Xin, 1995; He et al., 2014), burial dolomitization (Su et al., 2011; Chen et al., 2018; Fu et al., 2019), and localized hydrothermal dolomitization (Wang et al., 2009; Huang et al., 2011), which believe anhydrite contributes to forming high-quality reservoirs. The study area located in the central Ordos Basin, was initially considered to have low exploration potential due to poorly developed anhydrite and decreasing stratum thickness. However, high gas production from exploratory wells has spurred research into dolomite reservoir research in this region. Given the underdeveloped anhydrite sedimentation, the origin of dolomite reservoirs warrants further discussion. This study investigates the petrological characteristics and formation mechanism of dolomite for the Lower Ordovician Majiagou Formation in central Ordos Basin. Petrographic observations, X-ray diffraction (XRD) analyses and C–O–Sr isotopic data are used to characterize dolomite types and their petrological and geochemical features, clarifying the origin of dolomite reservoir, aiming to provide the geochemical and sedimentary dynamic evidence for predicting dolomite reservoirs in anhydrite-depleted settings and for guiding hydrocarbon exploration in similar basins globally.

2 Geological setting

Ordos Basin is a typical multi-cycle intracratonic basin located in the western North China Block (Figure 1a). It has six tectonic units, namely, the Weibei Uplift in the south, Yimeng Uplift in the north, Jinxi Fold Belt in the east, Yishan Slope in the central, Tianhuan Depression and the Western Margin Thrust Belt in the west (Fu et al., 2019; Cao et al., 2021; Tian et al., 2024). The study area is located in the central Ordos Basin, and in the middle of the Yishan Slope (Figure 1b).

Ten sub-members comprise the fifth member of Majiagou Formation, namely, $Ma5^1$ to $Ma5^{10}$. During the depositional period of the Ordovician Majiagou Formation, the basin experienced a protracted burial history and tectonic evolution. The "L" type paleo-uplift formed by subduction of Qingling-Qilian paleo-ocean crust controlled the sedimentary environment of the Ordos Basin, especially the central Ordos Basin (Figure 1c) (Zhou et al., 2023; Cao et al., 2018; Xi et al., 2017; Wang et al., 2009; Chen et al., 2020; Feng and Bao, 1999). Therefore, karstic reservoirs are deposited during $Ma5^1$ to $Ma5^4$ period, while dolomite and evaporite are characterized in $Ma5^5$ to $Ma5^{10}$ sub-member (Xiong et al., 2020; Mou et al., 2023 2020). Among them, the $Ma5^5$ and $Ma5^9$ were dominated by dolomite, while the $Ma5^6$, $Ma5^8$ and $Ma5^{10}$ formed thick gypsum-salt rock deposits (Zhou et al., 2023). However, affected by tectonic uplift, compared with the eastern Ordos Basin, the central Ordos Basin developed restricted platform sedimentary environment (Figure 1d), the lithology dominated by finely crystalline dolomite or finely to medium crystalline dolomite (Cao et al., 2021; Liu et al., 2020), rather than evaporites.

Specifically, when the rapid transgression cycles developed in the sub-members $Ma5^5$, $Ma5^7$ and $Ma5^9$, the sedimentary system of the restricted platform subfacies was developed. From west to east, dolomite flat, gypsum-bearing dolomite flat were developed successively. In addition, a gypsum-dolomite flat facies could be developed in a limited-range distribution. The lithology of the sediments mainly consists of dolomite, gypsum-bearing dolomite and gypsum-dolomite. While the sub-members $Ma5^6$, $Ma5^8$ and $Ma5^{10}$ are in the period of rapid marine regression cycles, the overall sedimentary facies characteristics and lithologies are similar to those of the sub-members $Ma5^5$, $Ma5^7$ and $Ma5^9$ in the period of rapid marine transgression cycles. The differences of sedimentary subfacies distribution are mainly related to the amplitude of sea oscillations (Yang et al., 2014; Yu et al., 2012; Shi et al., 2013; Wu et al., 2014) (Figure 1e).

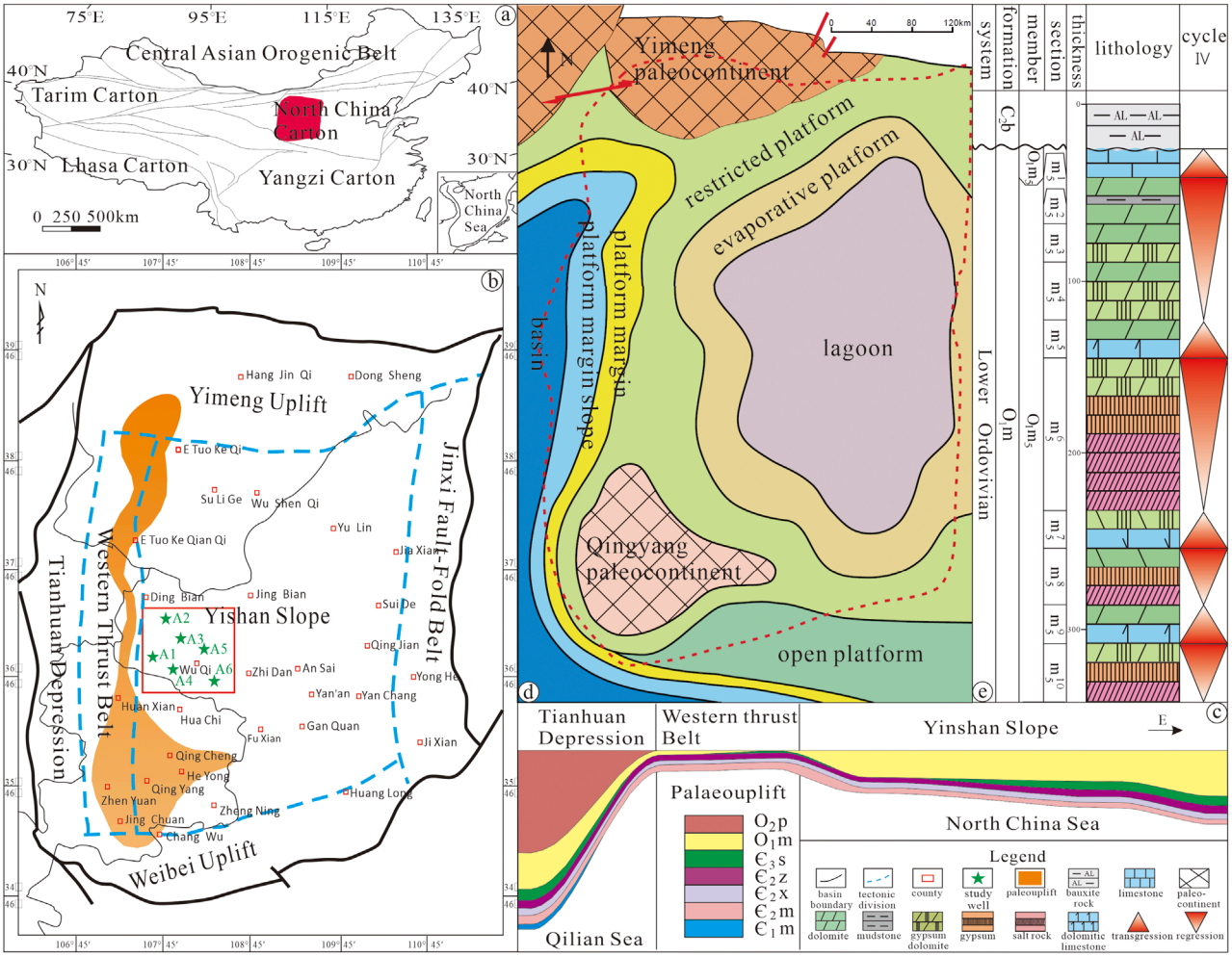

FIGURE 1
The structural, sedimentary, petrological column characteristics and the location of research area in the Ordos Basin, the red rectangle represents the study area. **(a)** The location of Ordos Basin in China; **(b)** the location of core samples in Ordos Basin; **(c)** geological structures evolution of regional geological structure; **(d)** sedimentary environment distribution during M_5^1 to M_5^{10} Formation; **(e)** the characteristics of lithology and sedimentary cycle column [reference from Zhou et al. (2023), Shi et al. (2021)].

3 Samples and experimental methods

The core samples of this study were collected from six coring wells in the Wu Qi areas of the Ordos Basin. Petrographic observations were conducted on all core samples, and 16 samples representing different dolomite types were selected for thin section, cathodoluminescence, XRD and C-O-Sr isotope analyses. In order to reflect the original sedimentary characteristics, and guarantee the accuracy of experiments results, we avoid dissolution holes and calcite veins to the largest extent during sampling.

3.1 Petrographic observation

There are 9 of 16 samples are made into thin section, which are doubly polished and half-stained with a mixture of Alizarin-red S and potassium ferricyanide to distinguish calcite and dolomite (Dickson, 1965; Fu et al., 2019; Cantrell et al., 2004). Besides, Cathodoluminescence (CL) analysis of five representative polished thin-sections was undertaken at Xi'an Petroleum University, China, using a CITL 8220 MK3 instrument (operating conditions: 20 kV beam voltage and 200 μA beam current).

3.2 XRD analysis

The Mg/Ca order degree and dolomite content determination can be obtained by XRD analysis. The Mg/Ca order degree was calculated based on the ratio of the reflection intensities of the diffraction peaks (015) (2θ = 35.3°) and (110) (2θ = 37.3°), as proposed by Füshtbauer and Goldschmidt in 1965, which can be used to indicate the degree of crystallization (Zhang et al., 2010; Manche and Kaczmarek, 2021). We put powdered samples into D2 Phaser diffractometer to analysis, with the detection standard SY/T-5163–1995. The results were obtained as weight percentages

TABLE 1 The petrological and mineralogical characteristics of the $Ma5^6$ to $M5^8$ Formation in the study area.

Sample	Form-ation	Litho-logy	The order degree	$\delta^{13}C$	Mean value	$\delta^{18}O$	Mean value	$^{87}Sr/^{86}Sr$	Mean value	Z value	Mean value
1	Ma_5^8	Md1	0.61	1.82		−5.33		0.70953		126.994	
2	Ma_5^8	Md1	0.53	1.18		−6.92		0.70971		126.270	
3	Ma_5^8	Md1	0.64	1.03		−5.58		0.70943		126.631	
6	Ma_5^8	Md1	0.67	−0.68	0.83	−5.88	−5.70	0.70983	0.70967	124.847	125.975
4	Ma_5^8	Md1	0.68	1.32		−5.26		0.70943		125.969	
5	Ma_5^8	Md1	0.79	0.81		−6.31		0.7098		125.816	
15	Ma_5^6	Md1	0.69	0.31		−5.30		0.70995		125.295	
7	Ma_5^7	Md2	0.83	−0.07		−6.68		0.70945		123.830	
9	Ma_5^7	Md2	0.87	−0.61		−8.10		0.70932		123.431	
10	Ma_5^7	Md2	0.81	−0.18		−7.05		0.70922		123.420	
11	Ma_5^7	Md2	0.81	−0.87		−6.03		0.70921		122.515	
13	Ma_5^6	Md2	0.98	−0.95	−0.48	−6.10	−7.12	0.70933	0.70946	122.316	122.878
8	Ma_5^7	Md2	0.93	0.03		−7.64		0.70922		124.433	
12	Ma_5^6	Md2	0.86	−0.99		−7.88		0.71062		121.348	
14	Ma_5^6	Md2	0.82	0.66		−6.51		0.70921		122.665	
16	Ma_5^6	Md2	0.78	−1.32		−8.10		0.70955		121.942	

of CaO and MgO, and final results are converted, calculated and present in Table 1.

3.3 Isotope analysis

16 Samples are powered for isotope analysis. For the carbon and oxygen isotope analysis, performed at the Geochemical Testing Department of Chinese Academy of Sciences using a Finnigan MAT252 (Ger many) mass spectrometer, samples are heated to remove organic matter and then release the CO_2 by reacting with anhydrous phosphoric acid under a vacuum at 25°C for 24 h. The testing basis was GB/T6041-2020 (Standard, 2020), and the isotope values were calculated according to the Peedee Belemnitella (PDB) standard (Sauer et al., 2001). Here, we also use the result of C-O isotope analysis to calculate Z value, which is a criteria to indicate the sedimentary environment by the equation:

$$Z = a(\delta^{13}C + 50) + b(\delta^{18}O + 50)$$

in which a and b are 2.048 and 0.498 respectively. The results of Z value are shown in Table 1, dolomite with a Z value above 120 would be classified as marine, those with Z value below 120 as continental (Li et al., 2014; Keith and Weber, 1964).

The Sr isotope analysis involved the following steps: (1) dissolving the powdered samples in ultrapure acid at 60°C for a duration of 24 h; (2) further separating the Sr using ion exchange resin; and (3) completing the analysis with a thermal ionization mass spectrometer (GV IsoProbe-T), achieving a high measurement accuracy.

4 Results

4.1 Dolomite petrography

There are various types of dolomites during $Ma5^6$ to $Ma5^8$ period in study area, the lithology distributed by micritic dolomite, fine-crystalline dolomite, and medium-crystalline dolomite according to the crystal size classification scheme (Huang, 2010; Sibley and Gregg, 1987). Here we recognized and focus on two types dolomite below by thin section observation and CL analysis as they widely distribution in the study area.

4.1.1 (Very) finely crystalline dolomite (Md1)

Md1 dolomite is well-developed in $M5^6$ and $M5^9$ Formation. In thin section, Md1 dolomite is gray or dark gray in colors

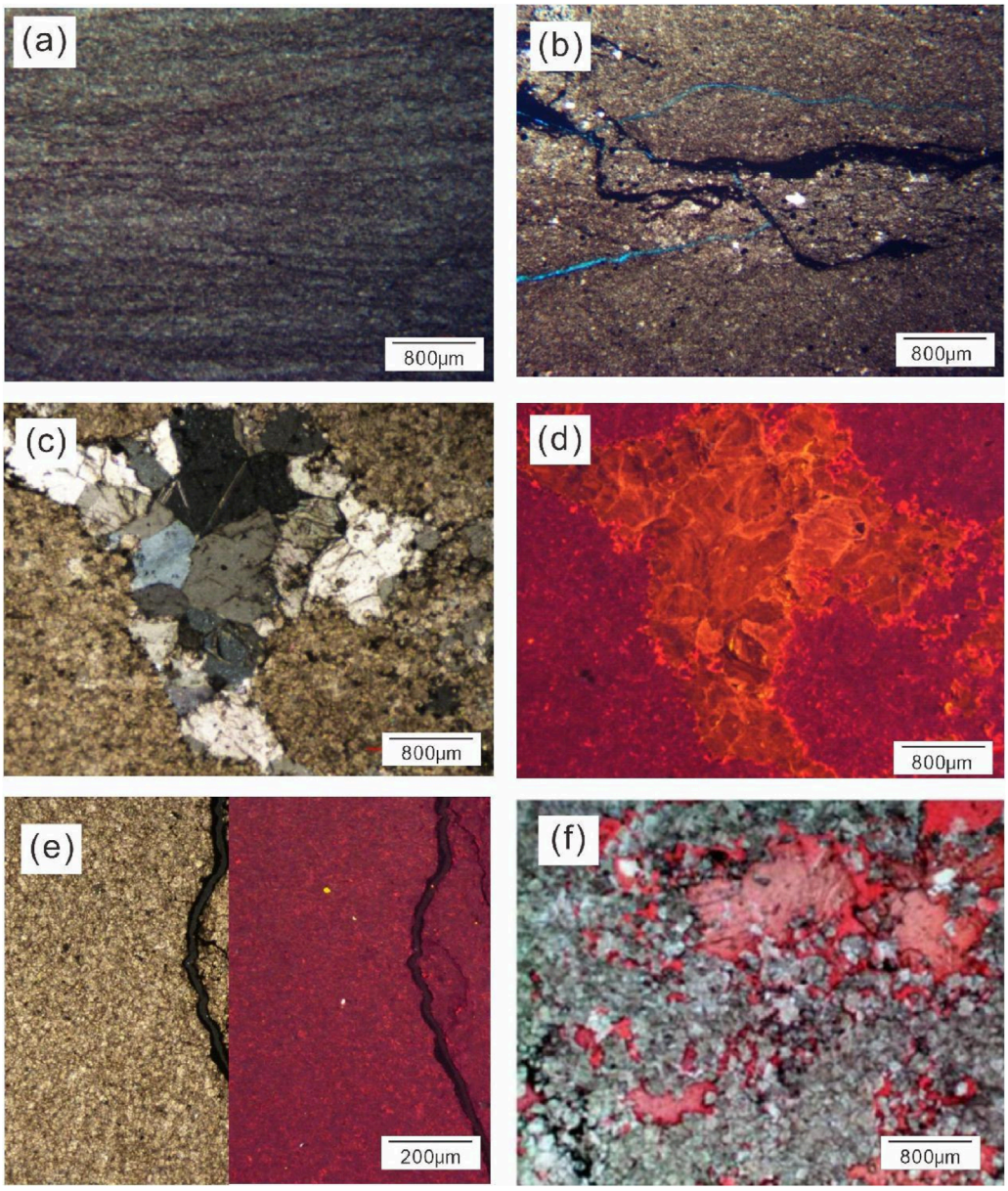

FIGURE 2
Petrographic features of Md1 dolomite during $M5^6$ to $M5^8$ formation in Ordos Basin. **(a)** Very finely crystalline dolomite, euhedral to subhedral, thin clay laminations, Well A3, 4089m; **(b)** very finely crystalline dolomite, microfracture (blue in color) or microfractures with organic matter filled (black in color), Well A2, 3,934.9m; **(c)** finely crystalline dolomite, dissolution pores filled by calcite, Well A3, 3,962.5m; **(d)** coupled CL photomicrograph of showing dull red luminescence of **(d)**, bright red luminescence of calcite, Well A3, 3,962.5m; **(e)** finely crystalline dolomite, coupled CL photomicrograph show dull red luminescence, Well A4 4,010.2m; **(f)** finely crystalline dolomite, crystalline size ranges relatively widely, dissolution pores generated, Well A1, 3,958.6 m.

(Figure 2), dolomite crystals are 5–20 μm in size, euhedral to subhedral of dolomite crystalline, featured by thin clay laminations (Figure 2a), micrite texture with organic matter filled (Figure 2b), dominated by microcrystalline or fine-crystalline structure and the crystal morphology is rather difficult to be identified. CL analysis shows a dull (Figure 2d) or dark red color (Figure 2e), and dissolution pores or filled by calcite can be observed occasionally (Figures 2c, f). It has the order degree of 0.53–0.79 (Table 1), with an average value is 0.65. The low value of order degree indicate that Md1 dolomite grows rapidly, lacking the conditions to form a crystalline structure. It likely that this type of dolomite was formed under weak to moderate hydrodynamic conditions, precisely in the tidal flat environment at the top of the upward shallowing cycle, being a product of the quasi syngenetic stage (Zhang et al., 2019; Warren, 2000; Sanz-montero et al., 2008).

4.1.2 Finely to medium crystalline dolomite (Md2)

Md2 dolomite is typically light brown, gray or light gray in color under thin section, with crystals size ranging from 20 to 60 μm,

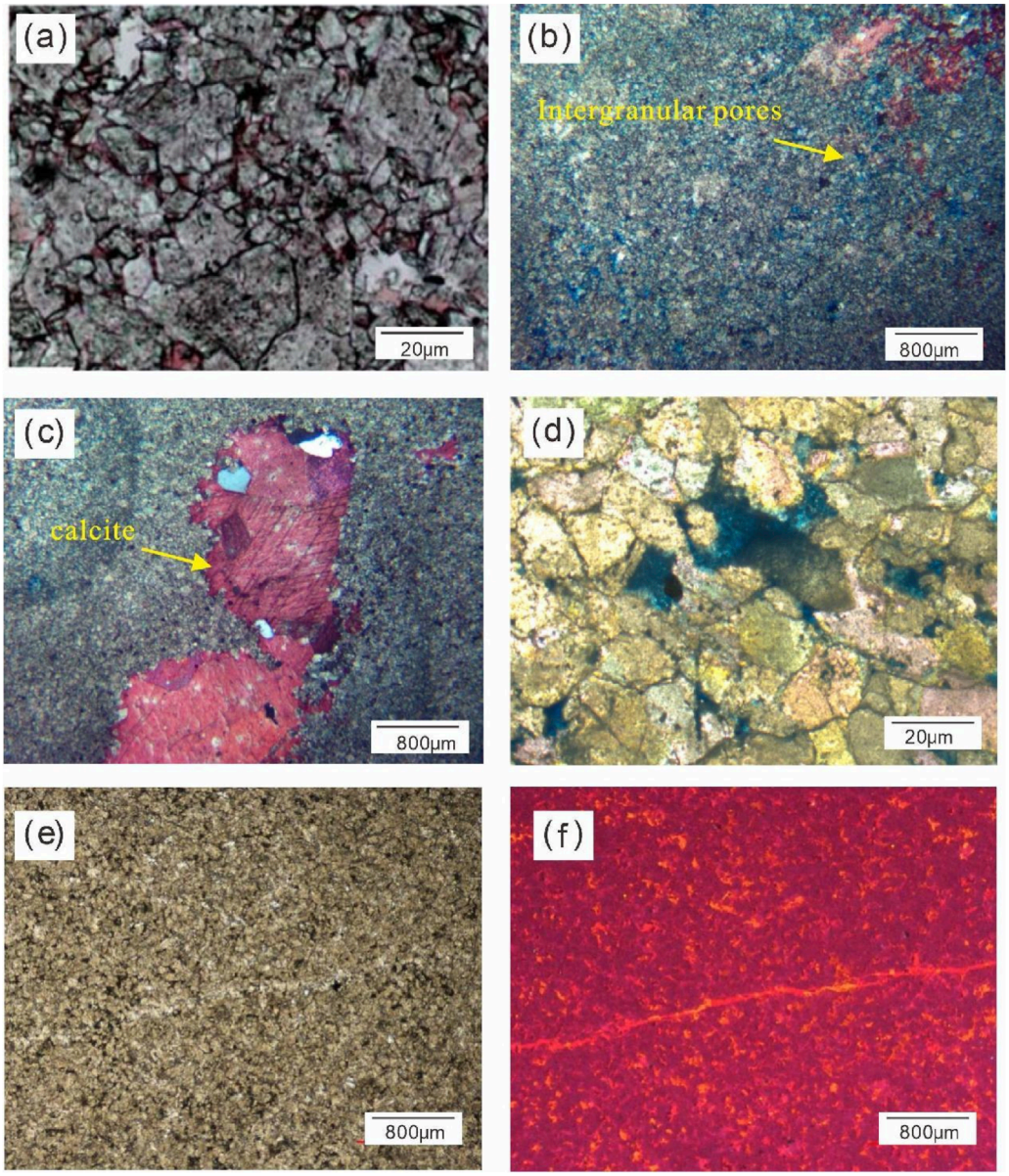

FIGURE 3
Petrographic features of Md2 dolomite. **(a)** Medium dolomite, euhedral to subhedral crystals, Well A4, 4,044.1m; **(b)** finely to medium dolomite, intercrystalline and dissolution pores developed, Well A2, 3,957.5m; **(c)** finely to medium dolomite, dissolution pores filled with calcite, Well A2, 3,957.5m; **(d)** medium dolomite, euhedral to subhedral crystals, inter-crystalline pores developed (blue color), Well A5 3,930.1m; **(e)** medium dolomite, micro-fracture can be observed, Well A5, 3,934.9m; **(f)** coupled CL photomicrograph of showing bright red luminescence of **(e)**, Well A3, 3,962.5 m.

which is widely developed in M_5^8 sub-member formation. It is observed to have fine to medium crystalline texture, with euhedral to subhedral crystals (Figure 3a). The dissolution or intergranular pores and fracture generated, some of them are filled with calcite can be occasionally seen (Figures 3b-e). Under CL, the Md2 dolomite displays dull or relatively bright red luminescence color (Figure 3f), and has the order degree of 0.78–0.98 (with an average value 0.85) (Table 1). The relatively high value of order degree indicates a sufficient conditions to form a crystalline structure to generate a higher euhedral degree. This type of dolomite is frequently observed in the tidal flat environment under weak hydrodynamic conditions and related to the reflux and percolation dolomitization during the shallow burial stage (Zhang et al., 2019; Warren, 2000; Su et al., 2011).

4.2 C-O isotopes

The stable isotope analysis results for carbon and oxygen are presented in Table 1 and Figure 4, which are commonly used for diagenetic fluid tracing (Major et al., 1992; Kaufman et al., 1993; Berra et al., 2020). In the study area, dolomite samples have $\delta^{13}C$ values of −1.32‰-1.82‰, with the average value is 0.11‰ (Md1 dolomite = −0.68‰ to +1.82‰, and Md2 dolomite =

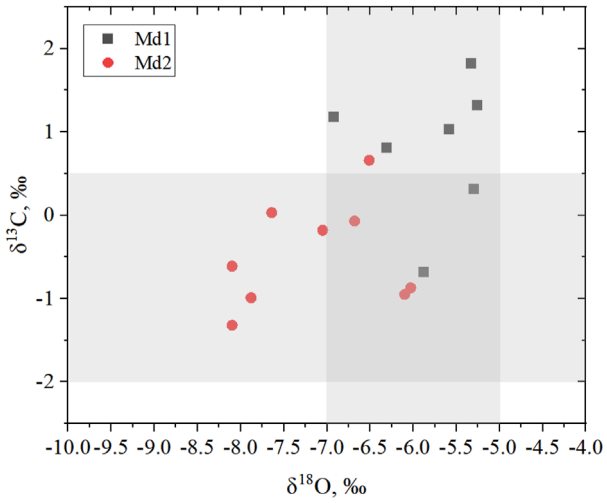

FIGURE 4
Cross-plot of $\delta^{13}C$ and $\delta^{18}O$ values in different dolomite types. The gray box represent Middle Ordovician marine calcite signature according to Veizer et al. (1999).

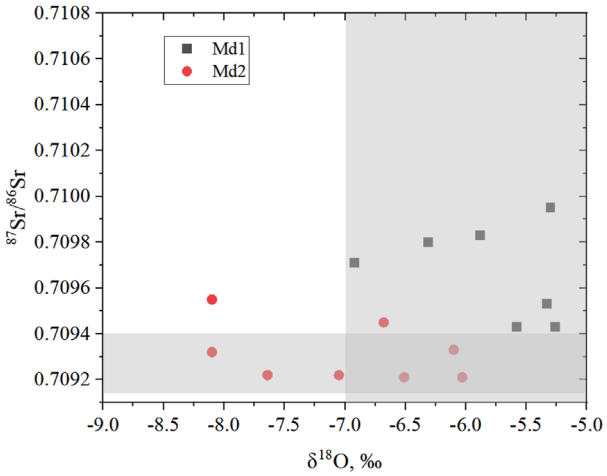

FIGURE 5
Cross-plot of $\delta^{18}O$ and $^{87}Sr/^{86}Sr$ values in different dolomite types. The gray box represent Middle Ordovician marine calcite signature according to Veizer et al. (1999).

−1.32‰–0.66‰), and $\delta^{18}O$ value of −8.1‰ to −5.26‰, with the average value is −6.54‰ (Md1 dolomite = −6.92‰ to −5.26‰, Md2 dolomite = −8.1‰ to −6.03‰). Previously measured C and O isotopes in the middle Ordovician seawater between −2.0‰ and +0.5‰ and −7‰ and −5‰, respectively (Allan and Wiggins, 1993; Bai et al., 2016). Therefore, samples of study area from M_5^6 to M_5^8 Formation basically fall within the range of carbon isotope, and display the slight negative oxygen isotope characteristics compared to the Ordovician seawater. In detail, the average $\delta^{13}C$ and $\delta^{18}O$ value of Md1 dolomite (mean value of $\delta^{13}C$ = +0.83‰, $\delta^{18}O$ = −5.79‰) is higher than that of Md2 dolomite (mean value of $\delta^{13}C$ = −0.48‰, $\delta^{18}O$ = −7.12‰).

4.3 Sr isotopes

Sixteen dolomite samples analyzed were also for Sr isotope test (Figure 5; Table 1). The $^{87}Sr/^{86}Sr$ ratios for the dolomite ranges from 0.70921 to 0.71062 (the average value is 0.70955). Besides, the $^{87}Sr/^{86}Sr$ value of Md1 dolomite is 0.70943–0.70995, with an average of 0.70967, Md2 dolomite has the $^{87}Sr/^{86}Sr$ ratios from 0.70921 to 0.71062 (average value is 0.70946, n = 9), which is lower than Md1 dolomite. Most of $^{87}Sr/^{86}Sr$ ratios from Md2 samples are higher than of the Middle Ordovician marine carbonate (between 0.7087 and 0.7092, from Veizer er al., 1999, Huang et al., 2011; Edwards et al., 2015), which may be associated with the presence of anhydrite (Su et al., 2011).

5 Discussion

5.1 Petrographic implications

Md1 dolomite is predominantly characterized by microcrystalline to subhedral dolomite crystals associated with anhydrite that has been replaced by calcite precipitation (Figure 2F). Previous studies have suggested that microcrystalline dolomite can form in evaporitic settings at relatively low temperatures (Gregg and Shelton, 1990; Fu et al., 2011; Loyd and Corsetti, 2010). The original limestone structure has been preserved within the microcrystalline dolomite, indicating its likely origin from near-surface dolomitization in a restricted, shallow environment during early diagenesis. Md1 dolomite pervasively replaces the matrix across all facies, especially in laminates where complete replacement occurs. The textures of Md1 dolomite and its close association with restricted-marine deposits suggest formation in a near-surface, low-temperature, saline environment with a high density of nucleation sites (Gregg and Shelton, 1990). Through petrographic observations, M1 dolomite is characterized by rich in terrigenous clay minerals, widely distributed in thin layers, and the bedding structure (Figure 2a) during the quasi-syngenetic dolomitization stage.

The Md2 dolomite is mainly composed of fine to medium-crystalline (30–100 μm), euhedral to subhedral dolomite crystals (Figure 3a), which preferentially replace the limestone matrix. The Md2 dolomite is characterized by partial to complete replacement of micritic limestone/silty limestone. This phenomenon indicates that there are a large number of replacement residues of micritic calcite or uncompletely dissolved micritic dolomite residues within the large crystals. The Md2 dolomite typically exhibits structural disruption and indistinct original sedimentary features. The high order degree (average value is 0.85) suggests that the concentration of magnesium ions in the fluid during dolomitization has decreased, and the replacement rate is relatively slow. Therefore, fine to medium dolomite crystals have formed, suggesting that Md2 dolomite formed during a period of shallow burial.

5.2 Petrogenesis of dolomite

C and O isotopes are commonly used for diagenetic fluid tracing as their compositions in the dolomite and the dolomitized rocks are closely related to the salinity and temperature of diagenetic

TABLE 2 Analysis of major and trace elements for various type of dolomite during the Ma_5^6 to Ma_5^9 period in the study area [Referenced from Yu (2019)].

Well	Type	ω/%			ω/10^{-6}				
		Fe_2O_3	Na_2O	K_2O	Mn	Ba	Sr	Pb	Zn
Y1112-1	Md1	0.25	0.02	0.08	69.02	11.23	63	0.26	3.31
Y1112-3		0.12	0.04	0.11	72.31	5.41	105.21	2.27	4.93
Y1112-4		0.13	0.04	0.06	78.52	3.53	93.94	0.66	2.41
Y1113-2		0.32	0.02	0.07	67.08	5.07	71.29	0.33	3.45
Y1165-6		0.38	0.04	0.03	83.93	16.26	86.38	0.5	2.48
Y1117-1	Md2	3.98	0.02	0.05	295.08	42.76	69.33	0.73	4.93
Y1112-7		2.68	0.02	0.89	43.37	28.56	88.6	2.6	6.97
Y1165-3		5.98	0.01	0.02	311.89	4.47	67.68	1.83	3.29

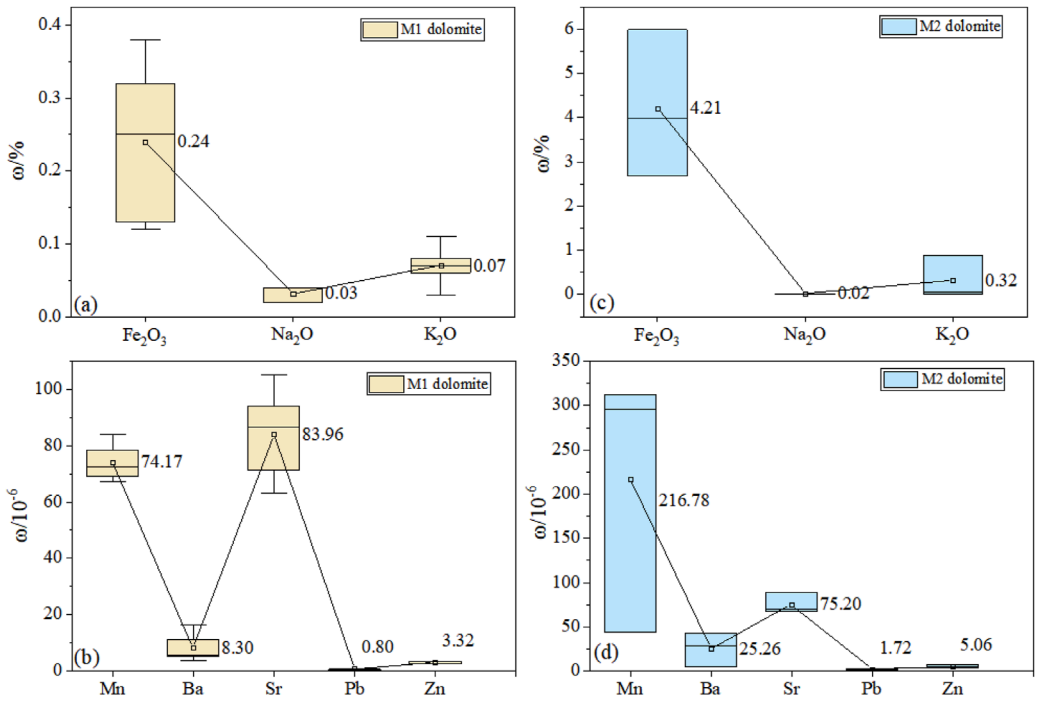

FIGURE 6
The characteristics of Major and Trace Elements in **(a, b)** Md1 and **(c, d)** Md2 dolomite of the Ordovician Majiagou Formation in the Study Area [Referenced from Yu (2019)].

fluids (Major et al., 1992; Kaufman et al., 1993; Berra et al., 2020). In addition, we use Keith and Weber's salinity index calculation formula Z to analyze diagenetic fluids. The ratio of $^{87}Sr/^{86}Sr$ can also reflect the information of diagenetic fluids, and thus is also widely used in the dolomite petrogenesis discussion (Wang et al., 2009).

5.2.1 Petrogenesis of Md1 dolomite

The results from C and O isotope tests of Md1 dolomite in the study area indicate the value of $\delta^{13}C$ is −0.68‰–1.82‰ (average value is 0.83‰), and $\delta^{18}O$ is −6.92‰ to −5.26‰ (average value is −5.79‰). Compared to C and O isotopes measurement value in the Ordovician seawater (Allan and Wiggins, 1993), Md1 dolomite samples have high $\delta^{13}C$ values and high anhydrite contents, which are likely to be related to evaporated seawater (Figure 4) (Wang et al., 2009; Shi et al., 2013; He et al., 2014). According to the O isotope value decreases gradually as the temperature rises (Zhao et al., 2005; Shields et al., 2003; Yu et al., 2012), it is deduced that strong evaporation, relatively shallow seawater, and the relatively high

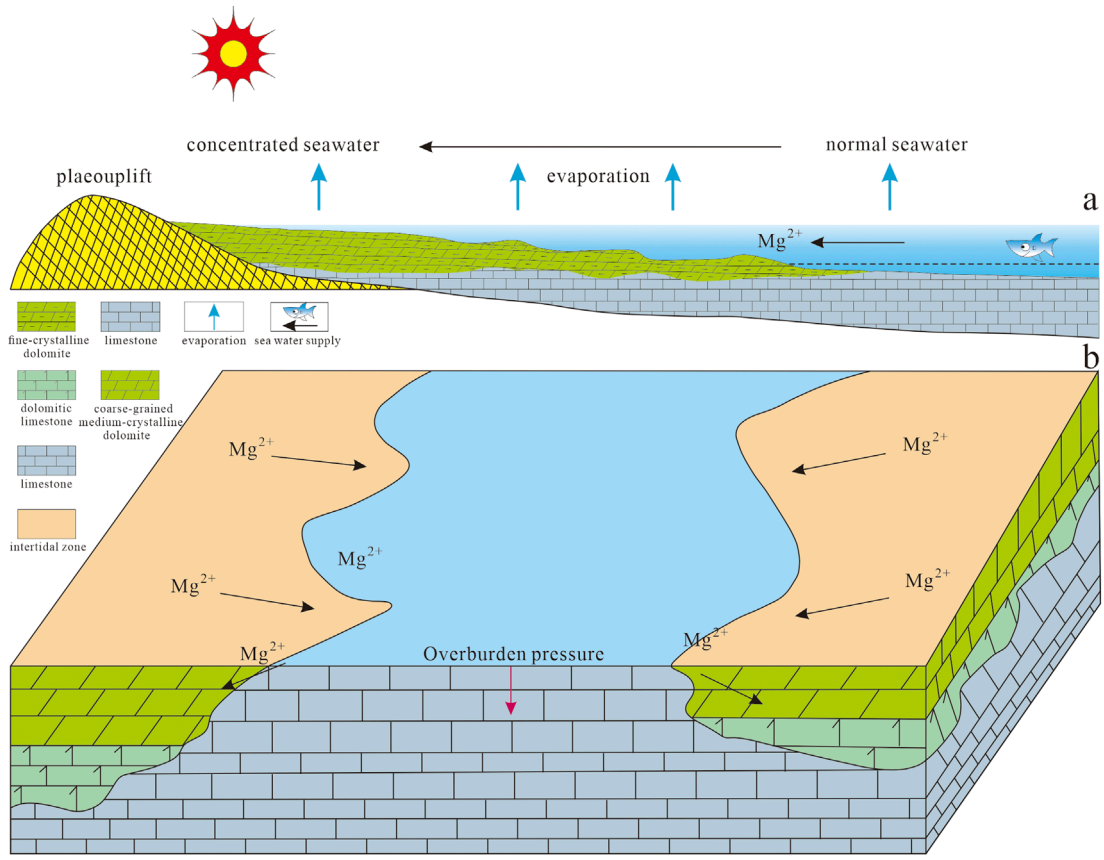

FIGURE 7
(a) The syngenetic-quasi syngenetic stages dolomitization model. **(b)** The shallow burial stage dolomitization model.

temperature depositional environment when the Md1 dolomite was formed, leading to the characteristics of slight negative oxygen isotope excursion (Figure 5). Meanwhile, the range of Z value from 124.84696 to 126.9936 with an average of 125.9747, indicating the dolomite should be formed in the high-salinity environment. The value of $^{87}Sr/^{86}Sr$ ratio is 0.70943–0.70995, and mean value is 0.70967 (Table 1), which is higher than those of contemporaneous seawater, indicating that the Md1 dolomite may be associated with the presence of anhydrite or the product of reflux and infiltration metasomatism by magnesium-rich concentrated brine from the tidal flat or overlying layers (Xiong et al., 2018; Su et al., 2011).

Moreover, according to the previous research results (Yu, 2019), the content of major and trace elements are relatively low, specifically, the average contents of major elements Fe, Na, and K are 0.24%, 0.03% and 0.07%, and the mean value of trace elements Mn, Ba, Sr, Pb and Zn are 74.14×10^{-6}, 8.3×10^{-6}, 83.97×10^{-6}, 0.8×10^{-6}, and 3.31×10^{-6} (Table 2). As shown in Figures 6a, b, the distribution characteristics of high value of Fe and Mn, and low value of Na and Sr indicating the Md1 dolomite was formed in a sedimentary environment with high salinity and restricted environment, and was influenced by atmospheric freshwater (Jiang et al., 2015; Bai et al., 2016; Yu, 2019). In addition, the low value of order degree and black-brown color in CL analysis (Figures 2d, e) also indicates the high-temperature environment. Therefore, the Md1 dolomite is formed from evaporated seawater after quasi syngenetic.

5.2.2 Petrogenesis of Md2 dolomite

The value of C isotope ranges from −1.32‰ to 0.66‰ with mean value is −0.48‰, which is equivalent to the $\delta^{13}C$ value of global seawater at the same time (Figure 4) (Veizer et al., 1999), indicating that the dolomitizing fluid was seawater-derived fluid. The $\delta^{18}O$ values of Md2 dolomite is −6.03‰ to −8.16‰, the average value is −7.12‰, which is lower than that of Md1 dolomite. Previous research indicates that the $\delta^{18}O$ values of dolomites formed in hydrothermal development environments are mostly less than −10.0‰ (Huang et al., 2011). The $\delta^{18}O$ values of the dolomite samples in the study area are all greater than −10.0‰ (Figure 5), eliminating the possibility of external hydrothermal fluid influence. The Z value is 121.3482–124.4332 with an average of 122.8781, being lower than that of Md1 dolomite, suggesting a reduction in dolomitization fluids salinity. In addition, the value of order degree is relatively high (mean value is 0.85) (Table 1), and the CL analysis Figure 3f shows a dark red or orange in color (Figure 1d) with the fine-crystalline grains can be observed. According to the relationship between C and O isotopes of dolomite and diagenesis proposed by James and Choquette (1986), it is held that Md2 dolomite should originally be the product of the deep burial stage. However, microscopic observations show that there is no saddle-shaped or coarse-grained dolomite in the study area.

The results of the major and trace element experiments indicate that, compared with Md1 dolomite, the contents of Fe (mean value

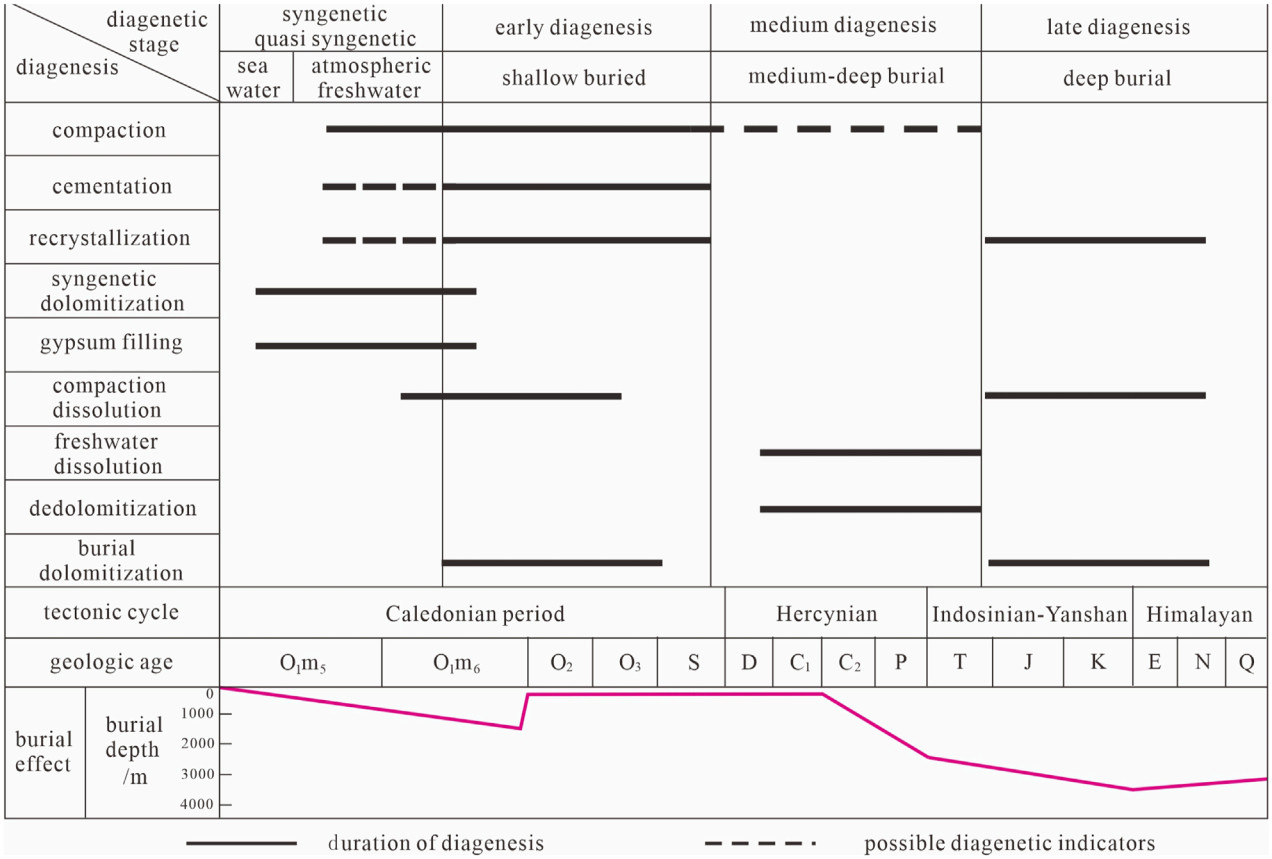

FIGURE 8
The diagenetic sequence of the Ma5^{6} to M5^{10} Formation in the study area [referenced from Su et al. (2011), Yu (2019)].

= 4.21%) and Mn (mean value = 283.45 × 10^{-6}) elements in Md2 dolomite are higher, and the content of Sr element is lower (mean value = 75.21 × 10^{-6}) (Figures 6c, d). The intensification of burial during diagenesis processes creates a reductive, high-temperature depositional environment that promotes Fe and Mn incorporation into the lattice. Besides, The decrease in Sr content during recrystallization is attributed to dolomite recrystallization (Ni et al., 2010; Kramer et al., 2001; Liu et al., 2020). This suggests that Md2 dolomite has progressed from the quasi syngenetic stage to the burial stage (Bai et al., 2016; Yu, 2019; Xiong et al., 2020), forming dolomite with larger grains and better self-consistency. The characteristics of larger crystalline grain can be observed in thin section (Figure 3a). Therefore, Md2 dolomite is interpreted as the product of shallow burial dolomitization.

5.3 Dolomitization mechanism and dolomites evolution

5.3.1 Dolomitization mechanism

During the lower and middle formation of the Middle Ordovician Majiagou period in the study area, the Ordos Basin near the equator experienced an arid climate with strong seawater evaporation and concentration (Bai et al., 2016; Chen et al., 2018; Fu et al., 2019).

Specifically, shallow-water carbonate platform tidal flat developed in the study area, increasing seawater salinity led to the development of high-frequency transgressive system cycle. It contributes primarily micritic limestone deposition, with only minor, discontinuous dolomite layers near the Yimeng ancient uplift (Figure 7a). In the later regression cycle, the study area featured a high-salinity, water-limited shallow sea environment dominated by evaporation. High-salinity seawater rapidly altered the early marlstone surface, forming thin, laterally unstable layers of quasi syngenetic micritic and fine-crystalline dolomite (Figure 7a). By the end of the sedimentation period of the Middle Ordovician Majiagou Formation, despite the shallow burial near the central paleo-uplift, the overall burial depth increased. This led to enhanced oxidation and higher formation temperatures. High-salinity, Mg^{2+}-rich seawater slowly seeped into the underlying unconsolidated limestone, displacing primary pore water and causing metasomatic dolomitization. This process formed thick, laterally stable, coarse-grained medium-crystalline dolomite, providing an ideal environment for natural gas accumulation in the Majiagou Formation (Figure 7b).

5.3.2 Dolomites evolution

Combining our petrological and geochemical experiment results and their implication with the depositional setting and burial history of the study area from previously research result. The

main types of diagenesis include dolomitization, filling, dissolution, cementation, recrystallization and dedolomitization in the study area during the Ma_5^6 to M_5^8 Formation (Yu, 2019; Shi et al., 2013). Four diagenetic stages have been experienced: the quasi-syndepositional near-surface to early diagenetic shallow burial diagenetic stage, the supergene atmospheric freshwater diagenetic stage, the middle diagenetic shallow-to-medium burial diagenetic stage, and the late diagenetic medium-to-deep burial diagenetic stage (Figure 8) (Su et al., 2011; Wu et al., 2014).

During the stage of quasi-syndepositional near-surface to early diagenetic shallow burial diagenetic stage, including compaction, the first stage of dolomitization, weak recrystallization, and cementation (Yu, 2019; Wu et al., 2014). The seawater with high-salinity, magnesium-rich in the dry, hot and restricted depositional environment, limestone or muddy limestone is transformed into micritic dolomite or finely crystalline dolomite through metasomatism. Subsequently, weak recrystallization prompted the grains of micritic dolomite or fine-crystalline dolomite to coarsen, forming fine-to medium-crystalline dolomite with larger intercrystalline pores (Figure 3b). Meanwhile, a part of carbonate grains were cemented by calcite, and evolved into dolomite through dolomitization (Liu et al., 2020; He et al., 2014).

Affected by the Caledonian movement, the study area experienced intermittent uplift. Although not exposed to the surface for a long time, the upper layers, which are closer to the weathering crust, have also suffered the erosion or dissolution of atmospheric freshwater during the exogenic period (Shi et al., 2013; Su et al., 2011). Therefore, a large number of dissolution pores, caves and fissures with irregular shapes are formed (Figure 3c), which increases the storage capacity of the dolomite reservoir.

During the medium burial diagenesis stage, the diagenetic processes mainly consist of dolomitization, organic acid dissolution, intense recrystallization, and filling (Xiong et al., 2020; Yu, 2019; Huang et al., 2014). The organic acid dissolution process enhance the reservoir capacity, making the dissolution pores, cavities, and fissures enlarge during the epigenetic period. Recrystallization, filling, compaction and pressure solution, cementation and metasomatism, severely damaged reservoir capacity, resulting in a significant reduction in pore volume, during the medium-deep burial diagenesis stage (Wu et al., 2014; Liu et al., 2020). However, exceptionally, the burial dolomitization has enhanced the euhedral degree of dolomite crystalline, providing a large number of intercrystalline pores (Figure 3b) and positive to the high-quality reservoirs develop.

6 Conclusion

(1) According to the classification scheme for the grain size of carbonate rocks, and considering the characteristics of petrography, two types of dolomite are mainly developed in the study area of the Yishan Slope in the Ordos Basin during M_5^6 to M_5^8 Formation, namely, (very) finely dolomite (Md1) and fine to medium crystalline dolomite (Md2). The Md1 dolomite characterized by microcrystalline (<20 μm), subhedral dolomite crystals, no or dull red in CL analysis. The Md2 dolomite is characterized by finely to medium-crystalline (20–60 μm), euhedral to subhedral dolomite crystals, with a dark red or orange in color by CL analysis.

(2) Based on systematic analysis of petrology, carbon-oxygen isotopes, major and trace elements from different types of dolomites, two main dolomitization processes were identified: quasi syngenetic and shallow burial reflux infiltration. The dolomitizing fluids were primarily marine-derived. Md1 dolomites formed in relatively open, low-oxidation, low-temperature conditions during the syngenetic-quasi syngenetic stage, while Md2 dolomites formed in the closed, low-reduction, higher-temperature conditions during shallow burial.

(3) A systematic investigation was carried out on the types of diagenesis in the study area, and the diagenetic sequence was established. The M_5^6 to M_5^8 Formation primarily exhibit dolomitization, filling, dissolution, cementation, recrystallization, and desulfatization. The Md1 dolomite induced to be associated with the presence of anhydrite or the product of reflux and infiltration metasomatism by magnesium-rich concentrated brine from the tidal flat or overlying layers, which is formed from evaporated seawater after quasi syngenetic. The Md2 dolomite dominated by a larger crystalline grain, a higher content of Fe and Mn, low content of Sr, indicating the stronger dolomitization and reductive sedimentary environment. Therefore, the Md2 dolomite is interpreted as resulting from shallow burial dolomitization.

Data availability statement

The original contributions presented in the study are included in the article/supplementary material, further inquiries can be directed to the corresponding author.

Author contributions

KT: Investigation, Writing–original draft, Writing–review and editing, Conceptualization, Methodology. JZ: Data curation, Investigation, Writing–original draft. XY: Data curation, Methodology, Writing–original draft. CX: Data curation, Investigation, Methodology, Writing–review and editing, Writing–original draft. JC: Data curation, Formal Analysis, Writing–review and editing. LM: Investigation, Writing–review and editing. WZ: Investigation, Writing – review and editing

Funding

The author(s) declare that financial support was received for the research and/or publication of this article. The project received funding from the Key R&D Plan of Shaanxi Province: Intelligent Evaluation Technology for Tight Gas Reservoir Driven by Data Mechanism Hybrid (Projects #2023-YBGY-308) and Investigation and Application of Microscopic Gas-Water Seepage Mechanisms in Tight Sandstone Reservoirs (Projects #2024ZC-KJXX-132).

Conflict of interest

Authors KT, JZ, XY, JC, LM, and WZ were employed by Shaanxi Yanchang Petroleum Group Co., Ltd.

Author CX was employed by PetroChina Changqing Oilfield Company.

Publisher's note

References

Allan, J. R., and Wiggins, W. D. (1993). *Dolomite reservoirs: geochemical techniques for evaluating origin and distribution*. American Association of Petroleum Geologists.

Bai, X. L., Zhang, S. N., Huang, Q. Y., Ding, X. Q., and Zhang, S. Y. (2016). Origin of dolomite in the Middle Ordovician peritidal platform carbonates in the northern Ordos Basin, western China. *Petroleum Sci.* 13, 434–449. doi:10.1007/s12182-016-0114-5

Berra, F., Azmy, K., and Della Porta, G. (2020). Stable-isotope and fluid inclusion constraints on the timing of diagenetic events in the dolomitized Dolomia Principale inner platform (Norian, Southern Alps of Italy). *Mar. Petroleum Geol.* 121, 104615. doi:10.1016/j.marpetgeo.2020.104615

Bontognali, T. R., Vasconcelos, C., Warthmann, R. J., Lundberg, R., and McKenzie, J. A. (2012). Dolomite-mediating bacterium isolated from the sabkha of Abu Dhabi (UAE). *Terra nova.* 24 (3), 248–254. doi:10.1111/j.1365-3121.2012.01065.x

Cantrell, D., Swart, P., and Hagerty, R. (2004). Genesis and characterization of dolomite, Arab-D reservoir, Ghawar field, Saudi Arabia. *Geoarabia-Manama* 9, 11–36. doi:10.2113/geoarabia090211

Cao, H. X., Li, W. H., Wu, H. Y., Wang, Z. G., Wu, Y., Ren, X. M., et al. (2021). Lithofacies palaeogeography evolution of the member 5 of Ordovician Majiagou sedimentary stage in northern Shaanxi province. *J. Palaeogeogr.* 23 (4), 723–734. doi:10.7605/gdlxb.2021.04.048

Cao, H. X., Shang, T., Wu, H. Y., Wang, N. X., and Feng, Y. (2018). Characteristics of carbon and oxygen isotopes of carbonate rocks in Majiagou Formation and their implication, southeastern Ordos Basin. *J. Northwest Univ.(Nat. Sci. Ed.)* 48, 578–586.

Chen, A. Q., Xu, S. L., Yang, S., Chen, H., Su, Z., Zhong, Y., et al. (2018). Ordovician deep dolomite reservoirs in the intracratonic Ordos Basin, China: depositional model and Diagenetic evolution. *Energy Explor. and Exploitation* 36 (4), 850–871. doi:10.1177/0144598718778171

Chen, A. Q., Zou, H., Ogg, J. G., Yang, S., Hou, M. C., Jiang, X. W., et al. (2020). Source-to-sink of Late carboniferous Ordos Basin: constraints on crustal accretion margins converting to orogenic belts bounding the North China Block. *Geosci. Front.* 11 (6), 2031–2052. doi:10.1016/j.gsf.2020.05.008

Davies, G. R., and Smith, L. B. (2006). Structurally controlled hydrothermal dolomite reservoir facies: an overview. *AAPG Bull.* 90 (11), 1641–1690. doi:10.1306/05220605164

Dickson, J. A. D. (1965). A modified staining technique for carbonates in thin section. *Nature* 205 (4971), 587. doi:10.1038/205587a0

Edwards, C. T., Saltzman, M. R., Leslie, S. A., Bergström, S. M., Sedlacek, A. R., Howard, A., et al. (2015). Strontium isotope ($^{87}Sr/^{86}Sr$) stratigraphy of Ordovician bulk carbonate: implications for preservation of primary seawater values. *GSA Bull.* 127 (9-10), 1275–1289. doi:10.1130/B31149.1

Feng, Z. Z., and Bao, Z. D. (1999). Lithofacies paleogeography of Majiagou age of ordoviccian in Ordos Basin. *Acta Sedimentol. Sin.* 17, 1–8.

Fu, J. H., Wang, B. Q., Sun, L. Y., Bao, H. P., and Xu, B. (2011). Dolomitization of ordovician Majiagou formation in Sulige region, Ordos basin. *Petroleum Geol. and Exp.* 33(3), 266–273. doi:10.11781/sysydz201103266

Fu, S. Y., Zhang, C. G., Chen, H. D., Chen, A. Q., Zhao, J. X., Su, Z. T., et al. (2019). Characteristics, formation and evolution of pre-salt dolomite reservoirs in the fifth member of the Ordovician Majiagou Formation, mid-east Ordos Basin, NW China. *Petroleum Explor. Dev.* 46 (6), 1153–1164. doi:10.1016/S1876-3804(19)60270-3

Garven, G., Appold, M. S., Toptygina, V. I., and Hazlett, T. J. (1999). Hydrogeologic modeling of the genesis of carbonate-hosted lead-zinc ores. *Hydrogeology J.* 7, 108–126. doi:10.1007/s100400050183

Gregg, J. M., and Shelton, K. L. (1990). Dolomitization and dolomite neomorphism in the back reef facies of the Bonneterre and Davis formations (Cambrian), southeastern Missouri. *J. Sediment. Res.* 60 (4), 549–562. doi:10.1306/212F91E2-2B24-11D7-8648000102C1865D

Han, Z., and Xin, W. J. (1995). Genetic mechanism and reservoir property of penecontemporary dolostones: the example of the major pay dolostons, Lower Paleozoic, Ordos region. *Earth Sci. Front. (China Univ. Geosci. Beijing)* 2 (3-4), 226–247.

He, X. Y., Shou, J. F., Shen, A. J., Wu, X. N., Wang, Y. S., H, Y. Y., et al. (2014). Geochemical characteristics and origin of dolomite: a case study from the middle assemblage of ordovician Majiagou Formation member 5 of the west of jingbian gas field, Ordos Basin, north China. *Petroleum Explor. Dev.* 41 (3), 417–427. doi:10.1016/S1876-3804(14)60048-3

Hsü, K. J., and Schneider, J. (1973). *Progress report on dolomitization hydrology of abu dhabi sabkhas, arabian gulf. The Persian gulf*. Berlin: Springer, 409–422.

Huang, S. J. (2010). *Carbonate diagenesis*. Beijing: Geological Publishing House, 1–288.

Huang, Z. C., and Bao, H. (2012). The characteristics of dolomite reservoir and trap accumulation in the middle assemblages of Ordovician in Ordos Basin, China. *Acta Pet. Sin.* 33 (S2), 118. doi:10.7623/syxb2012S2011

Huang, Z. L., Bao, H. P., Liu, J. F., Bai, H. F., and Wu, C. Y. (2011). Characteristics and genesis of dolomite in Majiagou Formation of ordovician, south of Ordos Basin. *Geoscience* 25 (5), 925–930.

Huang, Z. L., Liu, Y., Wu, C. Y., Wang, Q. P., and Ren, J. F. (2014). Characteristics of hydrocarbon accumulation in the middle and lower sections of middle assemblages of lower Ordovician Majiagou Member-5, Ordos Basin. *Mar. Orig. Pet. Geol.* 19 (3), 57–65. doi:10.3969/j.issn.1672-9854.2014.03.008

James, N. P., and Choquette, P. W. (1986). Diagenesis in limestones, 3. The deep burial environment. *Geosci. Can.* 14, 3–35.

Jiang, Y. Q., Liu, Y. Q., Yang, Z., Nan, Y., Wang, R., Zhou, P., et al. (2015). Characteristics and origin of tuff-type tight oil in jimusar depression, junggar basin, NW China. *Petroleum Explor. Dev.* 42 (6), 741–749. doi:10.1016/S1876-3804(15)30077-X

Jones, G. D., and Xiao, Y. (2005). Dolomitization, anhydrite cementation, and porosity evolution in a reflux system: insights from reactive transport models. *AAPG Bull.* 89 (5), 577–601. doi:10.1306/12010404078

Kaufman, A. J., Jacobsen, S. B., and Knoll, A. H. (1993). The Vendian record of Sr and C isotopic variations in seawater: implications for tectonics and paleoclimate. *Earth Planet. Sci. Lett.* 120 (3-4), 409–430. doi:10.1016/0012-821X(93)90254-7

Keith, M. L., and Weber, J. N. (1964). Carbon and oxygen isotopic composition of selected limestones and fossils. *Geochimica Cosmochimica Acta* 28, 1787–1816. doi:10.1016/0016-7037(64)90022-5

Kırmacı, M. Z., Yıldız, M., Kandemir, R., and Eroğlu-Gümrük, T. (2018). Multistage dolomitization in late jurassic–early cretaceous platform carbonates (berdiga formation), başoba yayla (trabzon), NE Turkey: implications of the generation of magmatic arc on dolomitization. *Mar. Petroleum Geol.* 89, 515–529. doi:10.1016/j.marpetgeo.2017.10.018

Kramer, W., Weatherall, G., and Offler, R. (2001). Origin and correlation of tuffs in the Permian Newcastle and Wollombi Coal Measures, NSW, Australia, using chemical fingerprinting. International Journal of Coal Geology, 47(2), 115–135. doi:10.1016/S0166-5162(01)00034-9

Li, Q. W., Jin, Z. K., and Jiang, F. J. (2014). Carbon and oxygen isotope analysis method for dolomite formation mechanism:A case study from Proterozoic dolomite in Yanshan area. *Lithol. Reserv.* 26 (4), 117–122.

Liu, M., Xiong, Y., Xiong, C., Liu, Y., Liu, L., Xiao, D., et al. (2020). Evolution of diagenetic system and its controls on the reservoir quality of pre-salt dolostone: the case of the Lower Ordovician Majiagou Formation in the central Ordos Basin, China. *Mar. Petroleum Geol.* 122, 104674. doi:10.1016/j.marpetgeo.2020.104674

Loyd, S. J., and Corsetti, F. A. (2010). The origin of the millimeter-scale lamination in the Neoproterozoic lower Beck Spring Dolomite: implications for widespread, fine-scale, layer-parallel diagenesis in Precambrian carbonates. *J. Sediment. Res.* 80 (7), 678–687. doi:10.2110/jsr.2010.063

Major, R. P., Lloyd, R. M., and Lucia, F. J. (1992). Oxygen isotope composition of Holocene dolomite formed in a humid hypersaline setting. *Geology* 20 (7), 586–588. doi:10.1130/0091-7613(1992)020<0586:OICOHD>2.3.CO;2

Manche, C. J., and Kaczmarek, S. E. (2021). A global study of dolomite stoichiometry and cation ordering through the phanerozoic. *J. Sediment. Res.* 91 (5), 520–546. doi:10.2110/jsr.2020.204

Mou, C. G., Xu, J., Gu, Y. H., Jia, J. P., and Wang, W. X. (2023). Reservoir characteristics and main controlling factors of the fourth member of Ordovician Majiagou Formation in the central and eastern Ordos Basin. *Petroleum Geology & Experiment*, 45(4), 780–790. doi:10.11781/sysydz202304780

Ni, S. Q., Hou, Q. L., Wang, A. J., and Ju, Y. W. (2010). Geochemical characteristics of carbonate rocks and its geological implications: taking the Lower Palaeozoic carbonate rock of Beijing area as an example. *Acta Geologica Sinica*, 84(10), 1510–1516.

Özyurt, M., Kandemir, R., and Yıldızoğlu, S. (2023). Geochemistry of the turonian-coniacian strata: new insight into paleoenvironmental conditions of the tethys, eastern pontides, NE Türkiye. *J. Asian Earth Sci.* 10, 100156. doi:10.1016/j.jaesx.2023.100156

Özyurt, M., and Kırmacı, M. Z. (2024). Microfacies and geochemistry of Kimmeridgian limestone strata in the Eastern Pontides (North-East Turkey): palaeoclimate and palaeoenvironmental influence on organic matter enrichment. *Depositional Rec.* 11, 4–21. doi:10.1002/dep2.286

Rahim, H. U., Qamar, S., Shah, M. M., Corbella, M., Martín-Martín, J. D., Janjuhah, H. T., et al. (2022). Processes associated with multiphase dolomitization and other related diagenetic events in the jurassic samana suk formation, himalayan foreland basin, NW Pakistan. *Minerals* 12 (10), 1320. doi:10.3390/min12101320

Sanz-Montero, M. E., Rodríguez-Aranda, J. P., and Garcia Del Cura, M. A. (2008). Dolomite–silica stromatolites in Miocene lacustrine deposits from the Duero Basin, Spain: the role of organotemplates in the precipitation of dolomite. *Sedimentology* 55 (4), 729–750. doi:10.1111/j.1365-3091.2007.00919.x

Sauer, P. E., Miller, G. H., and Overpeck, J. T. (2001). Oxygen isotope ratios of organic matter in arctic lakes as a paleoclimate proxy: field and laboratory investigations. *J. Paleolimnol.* 25, 43–64. doi:10.1023/A:1008133523139

Shi, B., Liu, Y., Wu, C., Huang, Z., and Ren, J. (2013). Geological conditions for hydrocarbon accumulation in middle reservoir-source rock combination of the Ordovician Majiagou Formation on the east side of the paleo-uplift in Ordos Basin. *Oil and Gas Geol.* 34 (5), 610–618. doi:10.11743/ogg20130505

Shi, J. A., Shao, Y., Zhang, S. C., Fu, C. Q., Bai, H. F., Ma, Z. L., et al. (2009). Lithofacies paleogeography and sedimentary environment in ordovician Majiagou Formation, eastern Ordos Basin. *Nat. Gas. Geosci.* 20 (3), 316–324.

Shi, P. P., Xiao, A. C., Fu, J. H., Wu, L., Zhou, Y. J., Wang, Y. P., et al. (2021). The sedimentary and tectonic framework of the Ordovician foreland basin in the southern margin of the Ordos Block and its evolution. *Acta Petrol. Sin.* 37 (8), 2531–2546. doi:10.18654/1000-0569/2021.08.17

Shields, G. A., Carden, G. A., Veizer, J., Meidla, T., Rong, J. Y., and Li, R. Y. (2003). Sr, C, and O isotope geochemistry of Ordovician brachiopods: a major isotopic event around the Middle-Late Ordovician transition. *Geochimica Cosmochimica Acta* 67 (11), 2005–2025. doi:10.1016/S0016-7037(02)01116-X

Sibley, D. F., and Gregg, J. M. (1987). Classification of dolomite rock textures. *J. Sediment. Res.* 57 (6), 967–975. doi:10.1306/212F8CBA-2B24-11D7-8648000102C1865D

State Administration for Market Regulation of the People's Republic of China, National Standardization Administration of the People's Republic of China (2020). General rules for mass spectrometric analysis. GB/T 6041-2020, (ICS): 71.080.01. Beijing, China: State Administration for Market Regulation of the People's Republic of China, National Standardization Administration of the People's Republic of China.

Su, Z. T., Chen, H. D., Xu, F. Y., Wei, L. B., and Li, J. (2011). Geochemistry and dolomitization mechanism of Majiagou dolomites in ordovician, Ordos, China. *Acta Petrol. Sin.* 27 (8), 2230–2238.

Tian, K., Qiao, X. Y., Zhou, J. S., Xue, C. Q., Cao, J., Yin, X., et al. (2024). Pore structure characteristics and influencing factors of dolomite reservoirs: a case study of the lower Ordovician Majiagou Formation, Ordos Basin, China. *Front. Earth Sci.* 12, 1407967. doi:10.3389/feart.2024.1407967

Veizer, J., Ala, D., Azmy, K., Bruckschen, P., Buhl, D., Bruhn, F., et al. (1999). $^{87}Sr/^{86}Sr$, $\delta^{13}C$ and $\delta^{18}O$ evolution of Phanerozoic seawater. *Chem. Geol.* 161 (1-3), 59–88. doi:10.1016/S0009-2541(99)00081-9

Wang, B. Q., Qiang, Z. T., Zhang, F., Wang, X. Z., Wang, Y., and Cao, W. (2009). Isotope characteristics of dolomite from the fifth member of the ordovician Majiagou Formation, the Ordos Basin. *Geochimica* 38 (5), 472–479.

Warren, J. (2000). Dolomite: occurrence, evolution and economically important associations. *Earth-Science Rev.* 52 (1-3), 1–81. doi:10.1016/S0012-8252(00)00022-2

Wu, D. X., Wu, X. N., Cao, R. R., and Yu, Z. (2014). Reservoir characteristics and evolution of Majiagou middle assemblage on east side of Ordovician central paleouplift, Ordos Basin. *Mar. Orig. Pet. Geol.* 19 (4), 38–44. doi:10.3969/j.issn.1672-9854.2014.04.006

Xi, S. L., Xiong, Y., Liu, X. Y., Lei, J. C., Liu, M. J., Liu, L., et al. (2017). Sedimentary environment and sea level change of the subsalt interval of Member 5 of Ordovician Majiagou Formation in central Ordos Basin. *J. Palaeogeogr.* 19 (5), 773–790. doi:10.7605/gdlxb.2017.05.061

Xiong, L., Yao, G., Xiong, S., Wang, J., Ni, C., Shen, A., et al. (2018). Origin of dolomite in the middle devonian guanwushan Formation of the western sichuan basin, western China. *Palaeogeogr. Palaeoclimatol. Palaeoecol.* 495, 113–126. doi:10.1016/j.palaeo.2017.12.035

Xiong, Y., Tan, X., Dong, G., Wang, L., Ji, H., Liu, Y., et al. (2020). Diagenetic differentiation in the ordovician Majiagou Formation, Ordos Basin, China: facies, geochemical and reservoir heterogeneity constraints. *J. Petroleum Sci. Eng.* 191, 107179. doi:10.1016/j.petrol.2020.107179

Yang, H., Bao, H. P., and Ma, Z. R. (2014). Reservoir-forming by lateral supply of hydrocarbon: A new understanding of the formation of Ordovician gas reservoirs under gypsolyte in the Ordos Basin. *Natural Gas Industry B*, 1 (1), doi:10.1016/j.ngib.2014.10.00324-31

Yu, C. Y. (2019). Genesis and main controlling factors of the middle and lower dolomite of the Majiagou Formation in the wuqi-ganquan ordovician, yishan Slope,Ordos Basin. *Northwest Universty*.

Yu, Z., S, L. Y., Wu, X. N., Wu, D. X., Yao, X. H., and D, Z. C. (2012). Characteristics and controlling factors of the middle array of Ordovician Majiagou reservoirs to the west of Jingbian gasfield, Ordos Basin. *Mar. Orig. Pet. Geol.* 17 (4), 49. doi:10.3969/j.issn.1672-9854.2012.04.008

Zhang, F., Xu, H., Konishi, H., and Roden, E. E. (2010). A relationship between d 104 value and composition in the calcite-disordered dolomite solid-solution series. *Am. Mineralogist* 95 (11-12), 1650–1656. doi:10.2138/am.2010.3414

Zhang, X., Zhang, T., Lei, B. J., Zhang, J., Zhang, J., Zhao, Z. J., et al. (2019). Origin and characteristics of grain dolomite of ordovician Ma55 member in the northwest of Ordos Basin, NW China. *Petroleum Explor. Dev.* 46 (6), 1182–1194. doi:10.1016/S1876-3804(19)60272-7

Zhao, J. X., Chen, H. D., Zhang, J. Q., Liu, X. L., and Fu, S. T. (2005). Genesis mode of the fifth member of Majiagou Formation in the middle Ordos Basin. *Acta Pet. Sin.* 26 (5), 38. doi:10.7623/syxb200505008

Zhou, J. G., Li, R. M., Wu, D. X., Yu, Z., Zhang, J., Zhang, T., et al. (2023). Characteristics and exploration potential of subsalt gas-bearing system in Majiagou Formation of middle ordovician in the eastern Ordos Basin. *Nat. Gas. Ind.* 43 (3), 34–45. doi:10.3787/j.issn.1000-0976.2023.03.004

Zhu, G. S., Zhao, J. X., Shao, X. Y., Li, F. J., and Ji, M. M. (2014). Reservoir characteristics and controlling factors of M 5 5 Sub-member of Majiagou formation in the east of Sulige area. *J. Southwest Petroleum Univ. Sci. and Technol. Ed.* 36 (3), 45–53. doi:10.11885/j.issn.1674-5086.2013.12.19.02